AJNR

3D Time-Resolved MR Angiography (MRA) of the Carotid Arteries with Time-Resolved Imaging with Stochastic Trajectories: Comparison with 3D Contrast-Enhanced Bolus-Chase MRA and 3D Time-Of-Flight MRA

R.P. Lim, M. Shapiro, E.Y. Wang, M. Law, J.S. Babb, L.E. Rueff, J.S. Jacob, S. Kim, R.H. Carson, T.P. Mulholland, G. Laub and E.M. Hecht

AJNR Am J Neuroradiol 2008, 29 (10) 1847-1854
doi: https://doi.org/10.3174/ajnr.A1252
http://www.ajnr.org/content/29/10/1847

ORIGINAL RESEARCH

3D Time-Resolved MR Angiography (MRA) of the Carotid Arteries with Time-Resolved Imaging with Stochastic Trajectories: Comparison with 3D Contrast-Enhanced Bolus-Chase MRA and 3D Time-Of-Flight MRA

R.P. Lim
M. Shapiro
E.Y. Wang
M. Law
J.S. Babb
L.E. Rueff
J.S. Jacob
S. Kim
R.H. Carson
T.P. Mulholland
G. Laub
E.M. Hecht

BACKGROUND AND PURPOSE: Time-resolved MR angiography (MRA) offers the combined advantage of large anatomic coverage and hemodynamic flow information. We applied parallel imaging and time-resolved imaging with stochastic trajectories (TWIST), which uses a spiral trajectory to undersample *k*-space, to perform time-resolved MRA of the extracranial internal carotid arteries and compare it to time-of-flight (TOF) and high-resolution contrast-enhanced (HR) MRA.

MATERIALS AND METHODS: A retrospective review of 31 patients who underwent carotid MRA at 1.5T using TOF, time-resolved and HR MRA was performed. Images were evaluated for the presence and degree of ICA stenosis, reader confidence, and number of pure arterial frames attained with the TWIST technique.

RESULTS: With a consensus interpretation of all sequences as the reference standard, accuracy for identifying stenosis was 90.3% for TWIST MRA, compared with 96.0% and 88.7% for HR MRA and TOF MRA, respectively. HR MRA was significantly more accurate than the other techniques ($P < .05$). TWIST MRA yielded datasets with high in-plane spatial resolution and distinct arterial and venous phases. It provided dynamic information not otherwise available. Mean diagnostic confidence was satisfactory or greater for TWIST in all patients.

CONCLUSION: The TWIST technique consistently obtained pure arterial phase images while providing dynamic information. It is rapid, uses a low dose of contrast, and may be useful in specific circumstances, such as in the acute stroke setting. However, it does not yet have spatial resolution comparable with standard contrast-enhanced MRA.

Stroke has an estimated prevalence of 5.7 million (2.6%) adults in the United States, where it is the third most common cause of mortality.[1] Atherosclerotic carotid artery disease is an important risk factor for anterior circulation ischemic stroke. Imaging evaluation is essential for optimal management and stroke prevention, as demonstrated in studies of symptomatic[2,3] and asymptomatic populations.[4,5] Carotid dissection is another potential cause of anterior circulation ischemia, which also requires high-spatial-resolution imaging for definitive diagnosis.

Digital subtraction angiography (DSA) remains the gold standard for assessment of the cervical vasculature,[6] with excellent spatial and temporal resolution. However, risks include vascular injury, intracerebral complications, contrast nephrotoxicity, and exposure to ionizing radiation. Therefore, noninvasive techniques are typically used initially. Duplex Doppler sonography, CT angiography (CTA), and MR angiography (MRA) all have high but varying degrees of sensitivity and specificity, ranging from 70% to 99% for carotid stenosis detection.[7] Although sonography provides excellent dynamic information and spatial resolution, insonation window limitations restrict anatomic coverage. Similarly, long imaging times with time-of-flight (TOF) MRA also limit anatomic coverage. CTA and conventional arterial contrast-enhanced MRA offer extensive coverage but provide no dynamic information and are dependent on accurate timing for optimal visualization of the arterial tree.

3D time-resolved contrast-enhanced MR angiography (TR MRA) has been previously described.[8] TR MRA offers combined anatomic and hemodynamic information and obtains pure arterial and venous phase images consistently and rapidly without a timing run. More recently, the technique has been specifically applied to the extracranial carotid arteries using parallel imaging or keyhole imaging techniques.[9,10] In this study, we report the diagnostic accuracy of TR MRA of the extracranial internal carotid artery (ICA) acquired with a combination of parallel imaging (generalized autocalibrating partially parallel acquisition [GRAPPA])[11] and time-resolved imaging with stochastic trajectories (TWIST), a new view-sharing technique, which undersamples the periphery of *k*-space depending on the radial distance from the center of *k*-space.[12,13] We compared TR MRA with 3D high-resolution contrast enhanced MRA (HR MRA) and 3D TOF MRA.

Materials and Methods

Patient Population

The study was institutional review board–approved, and a waiver of consent was obtained for this Health Insurance Portability and Ac-

Received October 12, 2007; accepted after revision June 20, 2008.

From the Department of Radiology (R.P.L., M.S., E.Y.W., J.S.B., L.E.R., J.S.J., S.K., R.H.C., T.P.M., E.M.H.), NYU Langone Medical Center, New York, NY; Siemens Medical Solutions (G.L.), Malvern, Pa; and Mount Sinai Medical Center (M.L., R.H.C.), New York, NY.

Paper previously presented at: Annual Meeting of the American Society of Neuroradiology, June 9–14, 2007; Chicago, Ill.

Please address correspondence to Ruth P. Lim, MD, 560 First Ave, Tisch Hospital, HW-202, New York, NY 10016; e-mail: ruth.lim@nyumc.org

indicates article with supplemental on-line tables.

DOI 10.3174/ajnr.A1252

countability Act–compliant retrospective study. Thirty-two consecutive patients were identified from the radiology data base who underwent carotid MRA on a 1.5T magnet (Avanto; Siemens Medical Solutions, Erlangen, Germany) from November 2006 to March 2007. One patient was excluded secondary to extravasation of contrast during acquisition. Of the final cohort, there were 16 men and 15 women, with an age range of 21–89 years (mean age, 59.9 years). Clinical indications for MRA included transient ischemic attack or stroke ($n = 18$), known cervical atherosclerotic disease ($n = 5$), and dissection evaluation/follow-up ($n = 8$).

MR Imaging

Patients underwent carotid MRA with 3 MRA sequences: 3D TOF MRA, contrast-enhanced 3D TWIST MRA, and 3D HR MRA. GRAPPA[11] was used for all sequences, with an acceleration factor of 2 used for the TWIST sequence. An 8-channel neurovascular array coil was used.

TOF

TOF coverage was limited to the cervical common carotid artery and carotid bifurcation, acquired axially, whereas the other 2 sequences acquired a sagittal oblique slab from the aortic arch to the circle of Willis. Imaging parameters were as follows: TR, 25 ms; TE, 7.2 ms; flip angle, 25°; FOV, 230 × 230 mm; matrix, 314 × 448; 90 partitions; voxel size after zero-interpolation, 0.7 × 0.5 × 0.9 mm^3 (true voxel size, 0.7 × 0.5 × 1.4 mm); acceleration factor, 3; acquisition time, 2:47 minutes.

Time-Resolved Imaging with TWIST

A 6-mL bolus of gadopentetate dimeglumine (Gd-DTPA, Magnevist; Bayer, Wayne, NJ) was administered at 2 mL/s, followed by a 15-mL saline flush. Imaging parameters were the following: TR, 3.3 ms; TE, 1.3 ms; flip angle, 25°; rectangular field of view (rFOV), 246 × 375 mm; matrix, 210 × 320; 88 partitions; voxel size after zero interpolation, 1.2 × 1.2 × 1.2 mm^3 (true voxel size, 1.2 × 1.2 × 2.0 mm^3); acceleration factor, 2. Although detailed physics of the TWIST sequence are beyond the scope of this article, a brief description is provided. TWIST relies on partial *k*-space undersampling, with emphasis on more frequent sampling of the center of *k*-space (designated as region A), relative to the periphery of *k*-space (designated as region B). Region A governs image contrast and is updated more rapidly than region B, which governs fine image detail. Missing data points in B for each sequential dataset are obtained from adjacent B intervals as shown in Fig 1. *K*-space sampling occurs in a continuous spiral fashion that allows a full range of *k*-space coverage from the center to the periphery and updating of high-frequency at the same rate as low-frequency information, though not all points in B are sampled during each acquisition.

The user may select the percentage of the center of *k*-space (A), compared with the entire *k*-space volume that is sampled with every acquisition (controlling image contrast), and the percentage of data points in the periphery of *k*-space (B) sampled per acquisition, with subsequent savings in acquisition time, at the expense of fine detail.

Values of A = 10% and B = 15% were used for TWIST MRA in our series. The sequence had a temporal resolution of 3.9 seconds, interpolated to 1.95 seconds, with 9 sequential non-breath-hold datasets obtained (1 precontrast and 8 postcontrast). Automated subtraction and coronal and sagittal maximal intensity projection (MIP) images were scanner-generated for the TWIST sequence.

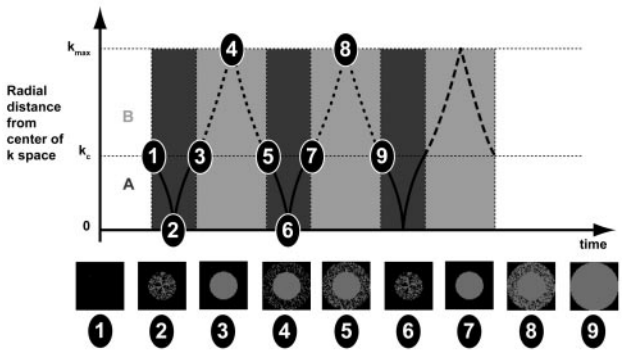

Fig 1. Diagram detailing the *k*-space trajectory used with the TWIST sequence, with a continuous sampling profile. Sampling commences 1) at the outer edge of the center region (A) of *k*-space, k_c and moves toward the center of *k*-space; 2) spirals back to k_c; 3) traverses a trajectory through the periphery (B) of *k*-space, moving out to the outer edge of *k*-space, k_{max} and then 4) back to k_c. 5) The cycle continues with the next iteration. The difference between iterations are the points of *k*-space sampled in B (points sampled for steps 7–9 differ from those sampled from 3–5). Therefore A is fully sampled with every iteration, but B requires 2 iterations in this schematic to be fully sampled, with subsequent gain in temporal resolution compared with conventional sampling of all points in *k*-space with each iteration. Filling of *k*-space is demonstrated at time points 1–9 at the bottom of the figure, with complete filling of *k*-space at time point 9.

Conventional HR MRA

For HR MRA, a 14-mL Gd-DTPA bolus and then a 20-mL saline flush was administered at 2 mL/s. Imaging parameters were the following: TR, 3.6 ms; TE, 1.4 ms; flip angle, 25°; rFOV, 234 × 375 mm; matrix, 256 × 512; 104 partitions; voxel size after zero interpolation, 0.9 × 0.7 × 1.0 mm^3 (true voxel size 0.9 × 0.7 × 1.6 mm^3); acceleration factor, 3. Three breath-hold acquisitions were obtained (1 precontrast and 2 postcontrast), with a timing run (1 mL of contrast) to obtain peak arterial enhancement in the ascending aorta on the first postcontrast acquisition, with a 7-second delay before the second postcontrast acquisition. The temporal resolution of each dataset was 18 seconds.

Image Evaluation

Two radiologists (with 1 year and 5 years' experience) interpreted studies in random order, blinded to patient history and identity, on a dedicated imaging workstation (Leonardo; Siemens Medical Solutions), where source, subtraction images and 3D multiplanar reformatting and MIP were available. A quantitative assessment of the greatest percentage of stenosis was made in each cervical ICA, by using North American Symptomatic Carotid Endarterectomy Trial guidelines[14] and by comparing the diameter of the most stenotic segment with the closest distal segment judged to be normal in caliber. Stenosis measurements were made from source data viewed in multiplanar reconstruction mode, with reference to subtraction images for TWIST and HR sequences as required. Stenoses were subsequently characterized into clinically relevant categories: mild (0%–49%), moderate (50%–69%), severe (70%–99%), or occluded (100%), for data analysis. Sequences were evaluated for diagnostic confidence on a 3-point scale (1 = poor, 2 = satisfactory, 3 = excellent). The TWIST sequence was evaluated for the number of arterial frames in which contrast was present at the carotid bifurcation before venous opacification.

Plaque surface morphology (1 = smooth, 2 = ulcerated) and dissection, if present, were recorded. Other vascular pathology affecting the vertebral, common carotid, and external carotid arteries was recorded, along with pathology of the aortic arch for the contrast-enhanced sequences. Artifacts hindering interpretation were noted. The reference standard was a consensus reading by both radiologists of all

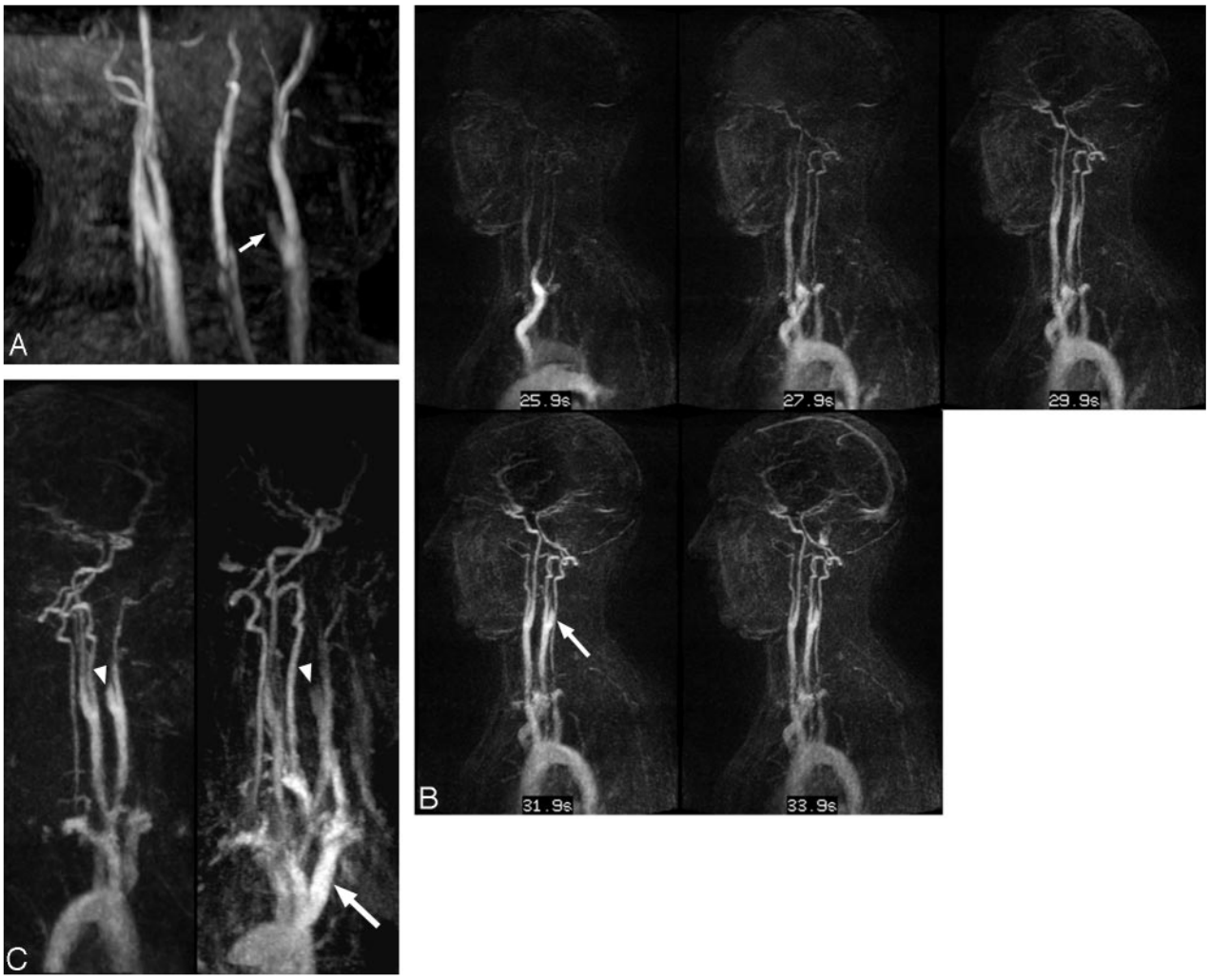

Fig 2. A 36-year-old woman (patient 13) presenting with right hemiparesis and left anterior circulation infarct diagnosed at brain MR imaging. *A,* TOF MIP (left anterior oblique projection) demonstrates tapering of the left ICA at the distal bulb level consistent with dissection (*arrow*). *B,* TWIST subtracted consecutive sagittal MIP images also demonstrate left ICA dissection (*arrow*), with delayed filling of the left carotid bulb in contrast to the right. Subsequent consecutive images (not shown) failed to show filling of the left ICA distal to the carotid bulb, and the left middle cerebral artery never opacified. *C,* Left anterior oblique subtraction MIP images from the TWIST (left) and HR (right) sequences demonstrate proximal left cervical ICA dissection (*arrowhead*). The HR sequence ia degraded by motion artifact and high-concentration contrast agent within the central veins (*arrow*).

3 sequences and DSA correlation, where available ($n = 2$, within 1 and 69 days of MRA without interval intervention).

A radiologist with 2 years' experience evaluated signal-intensity-to-noise ratio (SNR) and contrast-to-noise ratio (CNR) for each sequence (Appendix).

Statistical Analysis

Because all 3 sequences were used to derive data for each subject, statistical techniques appropriate for the analysis of correlated data were used to evaluate and compare the sequences. Specifically, the sequences were compared in terms of average reader confidence, SNR, and CNR by using a Wilcoxon matched-pairs signed rank test (ie, a Wilcoxon signed rank test applied to the within-subject differences between the sequences being compared). Logistic regression for correlated data (generalized estimating equations based on a binary logistic regression model[15]) was used to compare sequences for diagnostic accuracy relative to consensus opinion as the reference standard. For these comparisons, the stenosis grade for specific sequences was declared accurate only when in exact agreement with the consensus characterization. Stenoses outside the TOF MRA FOV were recorded as incorrect assessments for TOF MRA, by using the rationale that failure to diagnose a distal stenosis could negatively impact patient management.

Correlation between TWIST and TOF MRA and TWIST and HR MRA was calculated by using mixed-model regression analysis to account for statistical dependencies among observations provided by each reader for the same patient. Interobserver agreement for each sequence was measured by using the Cohen κ coefficient with linear weights. SAS Version 9.0 software (SAS Institute, Cary, NC) was used for all statistical computations. All reported *P* values are 2-sided and were declared statistically significant when $<.05$.

Results

Of 62 extracranial internal carotid arteries evaluated, 4 (6.5%) had 50%–69% stenosis, 1 (1.6%) had 70%–99% stenosis, and 2 (3.2%) were occluded according to the reference standard evaluation. This included 3 carotid dissections, where true luminal diameter was moderately stenotic to occluded (Fig 2). Ulcerated plaque was identified in 2 patients (Fig 3), whereas all other plaque was smooth.

The TWIST technique yielded datasets with distinct arte-

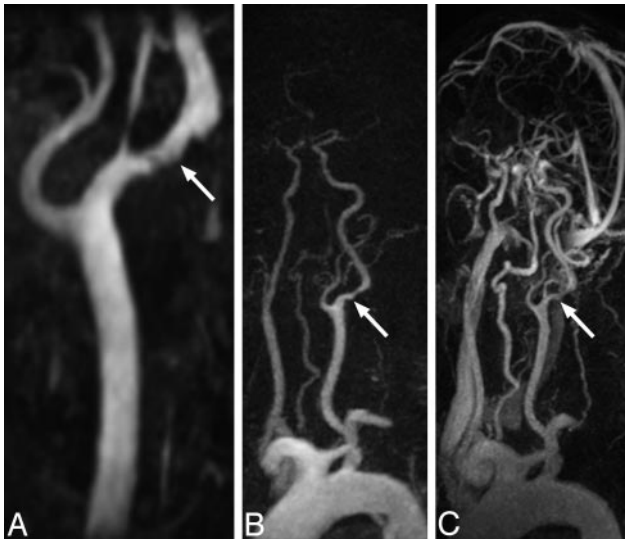

Fig 3. TOF MIP image (*A*), TWIST arterial phase subtracted MIP image (*B*), and HR MRA subtracted MIP image (*C*) demonstrate ulcerated plaque of the left ICA in an 80-year-old man (patient 4), causing mild (46%) stenosis (*arrows*). The degree of stenosis was overestimated by both readers using the TOF technique (73% and 65% for readers 1 and 2, respectively) and was accurately categorized for TWIST MRA (31% and 47%) and HR MRA (32% and 35%). TOF stenosis overestimation was attributed to in-plane saturation effects, because the proximal ICA is approaching the axial imaging plane in its orientation. Note the clear arterial phase image obtained by using the TWIST technique and the presence of venous contamination on the HR image.

rial and venous phases, with a mean and SD of 1.35 ± 0.52 pure arterial frames obtained for each patient.

Stenosis Evaluation

Overall, accuracy for stenosis assessment was greatest for HR MRA (96.0%), followed by TWIST (90.3%) and TOF MRA (88.7%), with significantly superior accuracy for HR MRA compared with both TWIST and TOF MRA ($P < .05$). There was no significant difference in accuracy between TWIST and TOF MRA ($P = .59$). On-line Table 1 summarizes results when data were divided into clinically relevant categories, with the highest accuracy of all individual sequences observed with mild stenosis and occlusion. High correlation between TWIST and TOF MRA ($r = 0.78$, $P < .001$) and TWIST and HR MRA ($r = 0.82$, $P < .001$) stenosis assessments was observed for all patients, and statistically significant correlation was also observed when analysis was restricted to patients with ≥50% stenosis (TWIST versus TOF MRA, $r = 0.70$, $P < .05$; TWIST versus HR MRA, $r = 0.73$, $P < .04$).

Severe Stenosis

The single case of severe stenosis was correctly identified with HR MRA and TOF MRA. The less experienced reader underestimated the severe stenosis with the TWIST technique. Severe stenosis was caused by a proximal ICA dissection and an adjacent intramural T1 hyperintense hematoma.

Moderate Stenosis

All sequences had relatively poor accuracy for moderate stenosis. For the TWIST technique, there were 3 incorrect readings. One was classified as incorrect because the stenosis was borderline moderate (69% at consensus interpretation, with the "incorrect" reading of 71% falling into the severe category). The other 2 were the following: 1) an overestimation of stenosis in a patient with remote dissection and recanalization of a complex dysplastic ICA; and 2) a moderate petrous left ICA stenosis missed by the less experienced reader, which was only identified by the second reader on the TWIST sequence and at the consensus reading. The stenosis was not identified by either reader at HR MRA due to venous contamination. For HR MRA, similar accuracy in the moderate stenosis group was demonstrated, with the petrous ICA stenosis described previously not identified by either reader due to adjacent venous signal intensity (SI) and 1 overestimation by 16% of a moderate stenosis by the less experienced reader. TOF MRA performed poorly (accuracy 12.5%) in the moderate stenosis group, with 2 stenoses outside the imaging FOV and an overestimation of stenosis in 1 case in which susceptibility artifact secondary to surgical clips was present.

Mild Stenosis

TWIST led to overestimation of mild stenoses in 5 cases. Cases in which discordant stenosis readings were recorded are detailed in On-line Table 2.

The 3 ICA dissections were identified on TWIST and HR MRA sequences in all cases. TOF MRA depicted the 2 proximal ICA dissections, with 1 dissection not seen because it was in the distal ICA, outside the imaging FOV.

Mean diagnostic confidence was satisfactory or greater for all 3 sequences: 2.61 ± 0.48, 2.29 ± 0.36, and 2.84 ± 0.37 for TOF, TWIST, and HR MRA respectively. Confidence with HR MRA was significantly higher compared with the other 2 sequences ($P < .04$) and, for TOF, was also significantly higher than that in TWIST ($P = .003$). SNR and CNR values were highest for HR MRA (which used 14 mL of Gd-DTPA), followed by TOF and then TWIST (6 mL of Gd-DTPA), as shown in On-line Table 3.

TWIST MRA also identified hemodynamic changes, with delayed filling of the carotid bulb in carotid dissection (Fig 2) and delayed opacification of a distal cervical internal carotid dissection following opacification of the circle of Willis (Fig 4), demonstrated with time-resolved MRA. Retrograde filling of a vertebral artery distal to an occlusion at its origin was also incidentally noted in 1 case. These findings were not apparent at HR MRA or TOF MRA.

There was greatest reader concordance for identifying each category of stenosis with the HR sequence (κ coefficient = 0.92), with substantial agreement also calculated for the TWIST and TOF MRA sequences ($\kappa = 0.73$ and 0.76, respectively).

Vessel-margin blurring was recorded for 30 of 31 patients for the TWIST sequence. In no case was motion artifact or venous contamination recorded. For TOF MRA, motion artifact ($n = 15$), wrap in the phase-encoding direction ($n = 9$), artifact related to flow turbulence ($n = 11$), and susceptibility artifact secondary to surgical clips ($n = 1$) were the factors hindering interpretation. For HR MRA, venous contamination was recorded in 16 patients, though diagnostic confidence remained satisfactory to excellent in 15 of these patients. Motion artifact ($n = 4$) and wrap in the phase-encoding direction ($n = 1$) also hindered interpretation of HR MRA.

Other pathology included vertebral artery steno-occlusive disease ($n = 5$) and severe (≥70%) common carotid artery

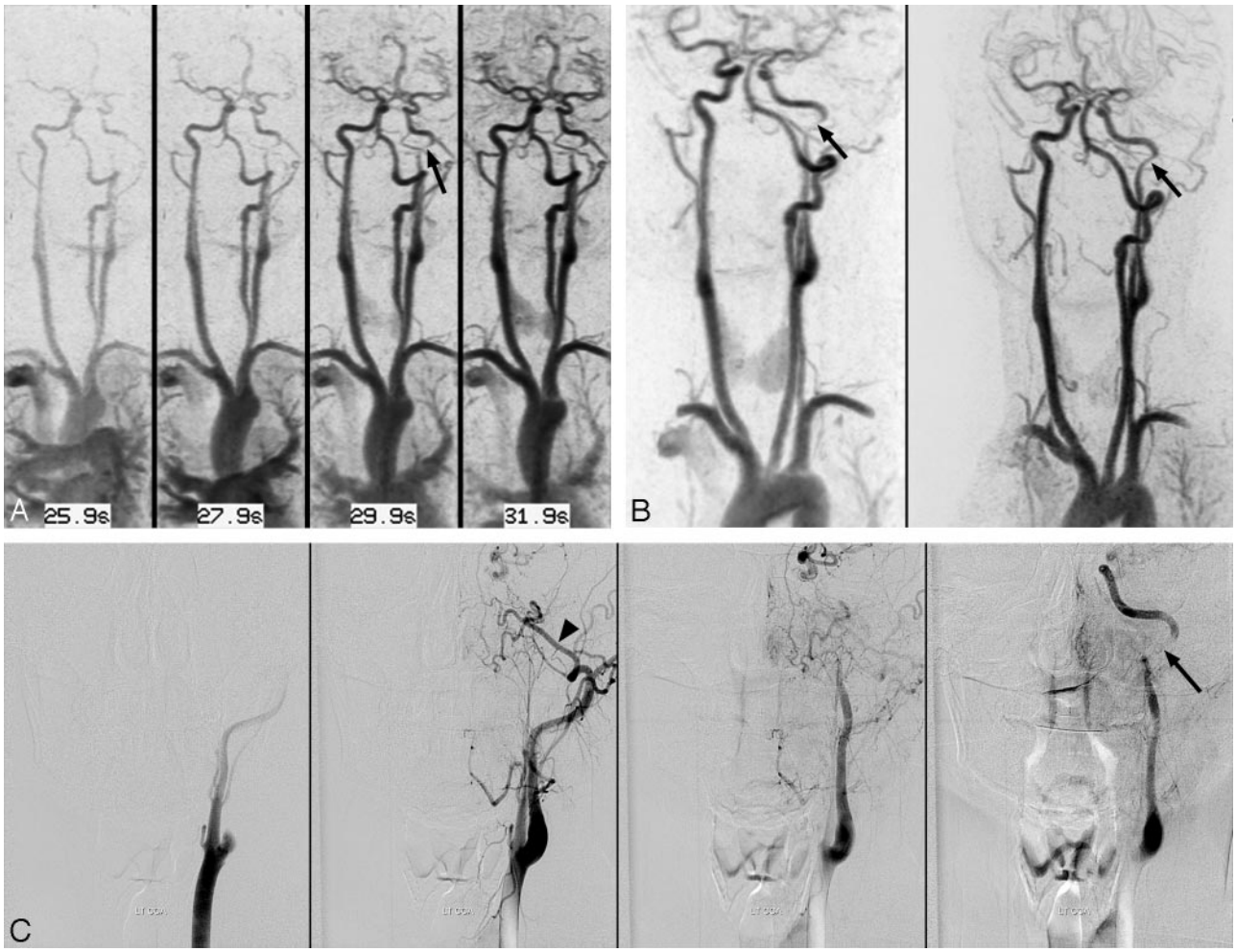

Fig 4. A 29-year-old woman (patient 2) presenting with neck pain. *A,* TWIST inverted MIP subtraction images in the coronal plane demonstrate the delayed appearance of a narrowed distal left cervical ICA (*arrow*), following the appearance of the intracranial left ICA and circle of Willis. *B,* TWIST (left) and HR inverted subtracted MIP image (right) in the left anterior oblique plane demonstrate an abnormal tapered appearance to the distal cervical left ICA (*arrows*). *C,* DSA images confirm a dissection of the distal left cervical ICA (*arrow*), reflected by delayed filling of the proximal left ICA in comparison with the left external carotid artery, best seen in the internal maxillary artery (*arrowhead*).

stenosis ($n = 2$). Common carotid artery stenosis was detected with high confidence in all sequences in both cases, and similarly, all vertebral artery steno-occlusive disease was detected with HR and TWIST MRA sequences. TOF MRA detected 60% (3/5) of vertebral artery disease, with 1 distal vertebral artery occlusion outside the imaging FOV and 1 proximal vertebral occlusion not detected, with TOF MRA images degraded by motion and wrap artifact in this patient.

DSA Correlation

DSA correlation was available in 2 patients. One patient had a complex dysplastic midcervical left ICA, recorded as a dissection causing severe stenosis on all 3 sequences and diagnosed as a remote dissection with recanalization versus a developmentally dysplastic artery at DSA. The second patient had a distal cervical left ICA dissection causing a moderate stenosis, remote bilateral vertebral artery dissections, and an incidental right ophthalmic artery aneurysm diagnosed only at conventional angiography. Both readers identified and accurately graded the ICA dissection on both TWIST and HR MRA sequences (Fig 4).

Discussion

Time-resolved MRA of the extracranial carotid arteries has been reported by using a fast low-angle shot 3D gradient-echo sequence with full sampling of *k*-space.[16,17] Time-resolved imaging has also been performed with spatial undersampling by using parallel imaging[9,18,19] and temporal undersampling techniques, such as time-resolved imaging of contrast kinetics (TRICKS),[8] or other alternatives[20,21] to achieve better temporal resolution.

A time-resolved sequence is beneficial in that it can be useful when there are differential rates of filling between normal and severely diseased cervical vessels or where there is collateral or retrograde flow in the setting of occlusion. The technique has potential value in the setting of carotid stent placement for assessment of altered hemodynamics, when stent-related susceptibility artifact may limit anatomic evaluation, and can also be useful to assess subclavian steal, hypervascular tumors, arteriovenous malformations, arteriovenous fistulas, or extracranial–intracranial bypasses.[22,23] Previously, only conventional angiography was available to provide a large FOV dynamic assessment. To our knowledge, this is the first description using the TWIST method of temporal undersam-

pling in combination with parallel imaging to assess the carotid circulation in symptomatic patients.

TWIST differs in the trajectory of *k*-space sampling compared with other temporal undersampling techniques described in the literature, such as TRICKS[8] and time-resolved echo-shared angiographic technique (TREAT).[24] Although all use a keyhole imaging approach to sample the center of *k*-space more frequently compared with high-spatial-frequency information peripherally, with TRICKS, *k*-space is divided into 1 central and several peripheral sections, with every iteration sampling the central section and 1 of the peripheral sections. TREAT differs in that alternating lines rather than different discrete sections of the periphery of *k*-space are sampled with each iteration, avoiding jumps between central and peripheral *k*-space data acquisition. TWIST uses a spiral and pseudostochastic rather than a linear trajectory to traverse a full range of *k*-space with every iteration, from center to periphery, on the basis of radial distance from the center of *k*-space (Fig 1), with theoretic advantages in image quality and reduction of artifacts. Although there have been reports in the literature studying different temporal undersampling techniques in this imaging region,[20,21,25] no direct comparisons of the techniques are available.

Our study showed that TWIST MRA has good accuracy at 1.5T with high correlation for stenosis estimation compared with established techniques. The transit time from the common carotid artery to the internal jugular vein is approximately 6–10 seconds.[26] Using a combination of spatial undersampling (GRAPPA) and temporal undersampling (TWIST) techniques, we achieved a temporal resolution of 3.9 seconds, allowing clear arterial datasets in every patient without a timing run. Another benefit of rapid acquisition time was that motion artifact, which hindered interpretation of both TOF and HR MRA sequences in our series, was almost completely eliminated. Additionally, near-isotropic datasets were obtained, allowing multiplanar reconstruction of images at consecutive timeframes.

The technique also demonstrated hemodynamic alterations, with delayed filling of the carotid bulb and distal cervical ICA in 2 cases of carotid dissection and retrograde filling of a proximally occluded vertebral artery evident only with time-resolved MRA. In contrast, TOF and conventional HR MRA only captures a single time point. Because subtraction images were available for interpretation, background SI could be eliminated and the small contrast dose used for this sequence still allowed satisfactory diagnostic confidence, which becomes of increasing importance given current concerns linking gadolinium chelates to nephrogenic systemic fibrosis in patients with severe renal impairment.[27]

The TWIST sequence demonstrated high accuracy comparable to TOF MRA and slightly inferior to HR MRA. The less experienced reader underestimated the only severe stenosis on the TWIST MRA in a patient in whom a T1 hyperintense intramural hematoma was adjacent to the stenosis. With regard to the incorrect TWIST MRA readings for moderate stenoses, 1 was underestimated by 2% (71% versus the consensus interpretation of 69%); therefore, it was incorrectly categorized in the severe category. The other 2 were a stenosis overestimation in a complex dysplastic ICA with remote dissection and a petrous ICA stenosis missed by the less experienced reader that was not identified at HR MRA by either reader due to venous contamination. As a result of this missed petrous ICA stenosis and an additional overestimation of TWIST MRA by the less experienced reader, HR MRA had accuracy similar to that of TWIST MRA in the moderate stenosis group. TOF MRA performed poorly in the moderate stenosis group, with factors including its limited FOV and clip susceptibility artifact causing stenosis overestimation in 1 case. The mild stenoses that were overestimated by TWIST MRA were attributed to poor definition of vessel margins, clip artifact, and misclassification of common carotid artery stenosis where plaque was crossing the carotid bifurcation.

It could be argued, however, that a shorter TE than that used in our study might have improved diagnostic accuracy of TOF MRA, because SI loss from turbulent flow may lead to overestimation of stenosis with increasing TE.[28] This likely contributed to the artifact from flow turbulence noted in 11 cases. However, a TE was used in our study that was similar to that reported previously for 3D TOF MRA of the carotid bifurcation.[18,29,30] Furthermore, TOF MRA may miss subtle luminal stenosis/plaques and vascular flaps from dissection that may be more apparent on intravenous contrast-enhanced MRA.

Although time-resolved MRA provides both dynamic and anatomic information, there are acknowledged disadvantages of loss of SNR from the parallel imaging (spatial undersampling) component and a trade-off between spatial and temporal resolution when temporal undersampling techniques are used. A specific limitation in our series was vessel blurring that was a feature of the TWIST sequence, likely due to overaggressive undersampling of high-spatial-frequency information, precluding optimal assessment of the degree of stenosis, with a tendency to overestimate mild stenosis (On-line Table 2). This likely also contributed to the relatively poor accuracy of the sequence in the moderate stenosis range. There is ongoing work to optimize the fraction of central (A) and peripheral (B) *k*-space sampled per iteration, tailored to the caliber of the vessel of interest. For example, identifying smaller vessels or differentiating complete occlusion from a residual hairline lumen will likely require a larger fractional sampling in each acquisition of both central *k*-space for contrast and peripheral *k*-space for fine detail.[31]

The low dose of contrast used for the TWIST sequence made comparison of SNR and CNR between sequences problematic and may also have decreased small-vessel conspicuity[32] in comparison with the higher dose HR MRA. Further, the short duration of the contrast bolus may have contributed to suboptimal vessel conspicuity.

A more general limitation was that readers could not be blinded to the sequence they were interpreting and sequences were performed in the same order in all patients. Only a relatively small number of patients in our series had severe disease, with only one 70%–99% stenosis and 2 occlusions, making it difficult to assess the true accuracy of the technique for severe stenosis. A larger prospective study with optimized TWIST parameters would allow further evaluation.

The study was also limited by lack of gold standard correlation, because only 2 of the 31 patients underwent DSA within 3 months of MRA; at our institution, management decisions are often based on sonographic or MRA findings, with

DSA reserved for further evaluation or consideration of endovascular management.

It has been reported that there are limitations to the degree of parallel imaging that can be used in combination with temporal undersampling techniques if images are to remain of diagnostic quality at 1.5T.[33] The technique would benefit from imaging at higher field strengths and extracellular contrast agents with higher relaxivity, such as gadobenate dimeglumine. This addition would allow greater SNR in the first instance and greater contrast and vessel conspicuity in the second. Higher parallel imaging factors could be used in conjunction with higher field strengths, where there is increased SI to "spend" on improvements in temporal and/or spatial resolution, as has been described with earlier time-resolved techniques.[20] Specific to carotid imaging, this would again be helpful in differentiating hairline residual patency of the cervical ICA from complete occlusion, with important management implications.

Conclusion

Time-resolved MRA with the TWIST sequence and parallel imaging at 1.5T using a low-contrast dose provides sufficient temporal resolution to assess the anatomy and hemodynamics of the extracranial carotid circulation. It can provide dynamic information noninvasively and rapidly, and delivers consistently pure arterial phase imaging. In its current form, TWIST imaging has potential use as a screening and supplementary tool. It may be particularly useful in the acute stroke setting, where rapid imaging helps limit motion artifact in circumstances where hemodynamic information is essential, such as differentiating critical stenosis from occlusion or when limiting contrast dosage is desirable. However, it does not yet have an accuracy comparable with the HR technique, due to artifacts related to temporal undersampling of *k*-space. With optimization of *k*-space sampling parameters, performance at higher field strengths, and use of newer gadolinium contrast agents, further improvements in temporal and spatial resolution are within reach.

Acknowledgment

We thank Dr. Randall Kroeker, PhD, of Siemens Medical Solutions, Malvern, Pa, for his invaluable technical expertise.

Appendix

SNR was estimated by using the following formula:

$$SNR = \frac{\textit{mean SI vessel region of interest (ROI)}}{\textit{SD of homogeneous tissue}}.$$

CNR was estimated by using the following formula:

$$\textit{CNR with parallel imaging} = \frac{(\textit{mean SI vessel ROI} - \textit{mean SI homogeneous tissue ROI})}{\textit{SD of homogeneous tissue}}.$$

Homogeneous tissue (subcutaneous fat) in close proximity to the vessel of interest was used to estimate noise because all 3 sequences used parallel imaging; therefore the use of air to calculate background noise was thought to be less accurate, given spatial variations in SNR with parallel imaging.[34]

In each case, a vessel ROI (terminal common carotid artery just proximal to carotid bifurcation) and subcutaneous fat ROI were obtained for 3 images in each dataset (TOF, arterial phase TWIST, and arterial phase HR MRA) on an imaging workstation (Leonardo, Siemens). SNR and CNR measurements were made, and the average of the 3 SNR and CNR measurements acquired was taken as the final SNR and CNR for each dataset.

References

1. Rosamond W, Flegal K, Furie K, et al, for the American Heart Association Statistics Committee and Stroke Statistics Subcommittee. **Heart disease and stroke statistics: 2007 update—a report from the American Heart Association Statistics Committee and Stroke Statistics Subcommittee.** *Circulation* 2007; 115;e172. Epub 2006 Dec 28
2. Gasecki AP, Eliasziw M, Ferguson GG, et al. **Long-term prognosis and effect of endarterectomy in patients with symptomatic severe carotid stenosis and contralateral carotid stenosis or occlusion: results from NASCET—North American Symptomatic Carotid Endarterectomy Trial (NASCET) Group.** *J Neurosurg* 1995;83:
3. **Randomised trial of endarterectomy for recently symptomatic carotid stenosis: final results of the MRC European Carotid Surgery Trial (ECST).** *Lancet* 1998;351:1379–87
4. **Endarterectomy for asymptomatic carotid artery stenosis: Executive Committee for the Asymptomatic Carotid Atherosclerosis Study**. *JAMA* 1995; 273:1421–28
5. Halliday A, Mansfield A, Marro J, et al. **Prevention of disabling and fatal strokes by successful carotid endarterectomy in patients without recent neurological symptoms: randomised controlled trial.** *Lancet* 2004;363:1491–502
6. Borisch I, Horn M, Butz B, et al. **Preoperative evaluation of carotid artery stenosis: comparison of contrast-enhanced MR angiography and duplex sonography with digital subtraction angiography.** *AJNR Am J Neuroradiol* 2003;24:1117–22
7. Brobeck BR, Forero NP, Romero JM. **Practical noninvasive neurovascular imaging of the neck arteries in patients with stroke, transient ischemic attack, and suspected arterial disease that may lead to ischemia, infarction, or flow abnormalities.** *Semin Ultrasound CT MR* 2006;27:177–93
8. Korosec FR, Frayne R, Grist TM, et al. **Time-resolved contrast-enhanced 3D MR angiography.** *Magn Reson Med* 1996;36:345–51
9. Golay X, Brown SJ, Itoh R, et al. **Time-resolved contrast-enhanced carotid MR angiography using sensitivity encoding (SENSE).** *AJNR Am J Neuroradiol* 2001;22:1615–19
10. Turski PA, Korosec FR, Carroll TJ, et al. **Contrast-enhanced magnetic resonance angiography of the carotid bifurcation using the time-resolved imaging of contrast kinetics (TRICKS) technique.** *Top Magn Reson Imaging* 2001; 12:175–81
11. Griswold MA, Jakob PM, Heidemann RM, et al. **Generalized autocalibrating partially parallel acquisitions (GRAPPA).** *Magn Reson Med* 2002;47:1202–10
12. Parrish T, Hu X. **Continuous update with random encoding (CURE): a new strategy for dynamic imaging.** *Magn Reson Med* 1995;33:326–36
13. Vogt FM, Eggebrecht H, Laub G, et al. *High spatial and temporal resolution MRA (TWIST) in acute aortic dissection: Proceedings of the International Society of Magnetic Resonance in Medicine,* Berlin, Germany: ISMRM; 2007. Berlin, Germany: May 19–25, 2007
14. **North American Symptomatic Carotid Endarterectomy Trial: methods, patient characteristics, and progress**. *Stroke* 1991;22:711–20
15. Zeger SL, Liang KY. **Longitudinal data analysis using generalized linear models.** *Biometrics* 1986;42:121–30
16. Remonda L, Senn P, Barth A, et al. **Contrast-enhanced 3D MR angiography of the carotid artery: comparison with conventional digital subtraction angiography.** *AJNR Am J Neuroradiol* 2002;23:213–19
17. Lenhart M, Framme N, Volk M, et al. **Time-resolved contrast-enhanced magnetic resonance angiography of the carotid arteries: diagnostic accuracy and inter-observer variability compared with selective catheter angiography.** *Invest Radiol* 2002;37:535–41
18. Fellner C, Lang W, Janka R, et al. **Magnetic resonance angiography of the carotid arteries using three different techniques: accuracy compared with intraarterial x-ray angiography and endarterectomy specimens.** *J Magn Reson Imaging* 2005;21:424–31
19. Meckel S, Mekle R, Taschner C, et al. **Time-resolved 3D contrast-enhanced MRA with GRAPPA on a 1.5-T system for imaging of craniocervical vascular disease: initial experience.** *Neuroradiology* 2006;48:291–99
20. Nael K, Michaely HJ, Villablanca P, et al. **Time-resolved contrast enhanced magnetic resonance angiography of the head and neck at 3.0 Tesla: initial results.** *Invest Radiol* 2006;41:116–24
21. Du J, Fain SB, Korosec FR, et al. **Time-resolved contrast-enhanced carotid**

imaging using undersampled projection reconstruction acquisition. *J Magn Reson Imaging* 2007;25:1093–99
22. Krings T, Hans F. **New developments in MRA: time-resolved MRA**. *Neuroradiology* 2004;46(suppl 2):s214–22
23. Tsuchiya K, Honya K, Fujikawa A, et al. **Postoperative assessment of extracranial-intracranial bypass by time-resolved 3D contrast-enhanced MR angiography using parallel imaging.** *AJNR Am J Neuroradiol* 2005;26:2243–47
24. Pinto C, Hickey R, Carroll TJ, et al. **Time-resolved MR angiography with generalized autocalibrating partially parallel acquisition and time-resolved echo-sharing angiographic technique for hemodialysis arteriovenous fistulas and grafts.** *J Vasc Interv Radiol* 2006;17:1003–09
25. Frydrychowicz A, Bley TA, Winterer JT, et al. **Accelerated time-resolved 3D contrast-enhanced MR angiography at 3T: clinical experience in 31 patients.** *MAGMA* 2006;19:187–95
26. Kim JK, Farb RI, Wright GA. **Test bolus examination in the carotid artery at dynamic gadolinium-enhanced MR angiography.** *Radiology* 1998;206:283–89
27. Grobner T. **Gadolinium: a specific trigger for the development of nephrogenic fibrosing dermopathy and nephrogenic systemic fibrosis?** *Nephrol Dial Transplant* 2006;21:1104–08
28. Lev MH, Romero JM, Gonzalez RG. **Flow voids in time-of-flight MR angiography of carotid artery stenosis? It depends on the TE!** *AJNR Am J Neuroradiol* 2003;24:2120
29. Lell M, Fellner C, Baum U, et al. **Evaluation of carotid artery stenosis with multisection CT and MR imaging: influence of imaging modality and post-processing.** *AJNR Am J Neuroradiol* 2007;28:104–10
30. Townsend TC, Saloner D, Pan XM, et al. **Contrast material-enhanced MRA overestimates severity of carotid stenosis, compared with 3D time-of-flight MRA.** *J Vasc Surg* 2003;38:36–40
31. Song T, Laine AF, Chen Q, et al. *A quantitative simulation approach for optimization of spiral k-space-sampled time-resolved contrast-enhanced MRA: Proceedings of the International Society of Magnetic Resonance in Medicine,* Berlin, Germany: ISMRM; 2007. Berlin, Germany: May 3–9, 2007
32. Frayne R, Grist TM, Swan JS, et al. **3D MR DSA: effects of injection protocol and image masking.** *J Magn Reson Imaging* 2000;12:476–87
33. Gauvrit JY, Law M, Xu J, et al. **Time-resolved MR angiography: optimal parallel imaging method.** *AJNR Am J Neuroradiol* 2007;28:835–38
34. Heverhagen JT. **Noise measurement and estimation in MR imaging experiments.** *Radiology* 2007;245:638–39